

Congenitally corrected transposition of the great arteries: is it really a transposition? An anatomical study of the right ventricular septal surface

Nicolas Arribard,^{1,2}  Meriem Mostefa Kara,^{1,3}  Sébastien Hascoët,^{2,3}  Bettina Bessières,⁴ Damien Bonnet^{5,6} and Lucile Houyel^{1,5,6}

¹Laboratory of Anatomy of Congenital Heart Disease - M3C, Hôpital Marie Lannelongue, Le Plessis-Robinson, France

²Laboratory of Surgical Research, INSERM U999, Hôpital Marie Lannelongue, Le Plessis Robinson, France

³Medico-surgical Unit, Congenital and Paediatric Cardiology, Centre de Référence Malformations Cardiaques Congénitales Complexes - M3C, Hôpital Marie Lannelongue, Le Plessis Robinson, France

⁴Fetal Pathology Department, Hôpital Necker Enfants Malades, APHP, Paris, France

⁵Université Paris Descartes, Sorbonne Paris Cité, Paris, France

⁶Medico-surgical Unit, Congenital and Paediatric Cardiology, Centre de Référence Malformations Cardiaques Congénitales Complexes - M3C, Hôpital Necker Enfants Malades, APHP, France

Abstract

Congenitally corrected transposition of the great arteries (ccTGA) is a rare congenital malformation which associates discordant atrioventricular and ventriculo-arterial connections. Although frequently associated with a ventricular septal defect (VSD), its anatomy remains controversial. This could be due in hearts with usual atrial arrangement to the apparently different anatomy of the left-sided right ventricle compared with a right-sided right ventricle. We wanted to compare the RV septal anatomy between ccTGA, transposition of the great arteries and normal heart and to determine the anatomy of the VSD in ccTGA. We analysed 102 human heart specimens: 31 ccTGA, 36 transpositions of the great arteries, 35 normal hearts. According to the last classification of VSD (ICD-11), VSD were classified as outlet if located above the superoseptal commissure of the tricuspid valve and inlet if underneath. We measured the lengths of the superior and inferior limbs of the septal band and the angle between the two limbs. To assess the orientation of the septal band, we also measured the angle between superior limb and the arterial valve above. A VSD was present in 26 ccTGA (84%) and was an outlet VSD in 16 cases (61%). The mean angle between the two limbs of the septal band was 76.4° for ccTGA compared with 90.6° for transposition of the great arteries ($P = 0.011$) and 76.1° for normal hearts ($P = NS$). The mean angle between the superior limb of the septal band and the arterial valve above was 70.6° for ccTGA compared with 90.6° for transposition of the great arteries ($P = 0.0004$) and 69.1° for normal hearts ($P = NS$). The inferior limb of the septal band was significantly shorter in ccTGA ($P < 0.0003$): SL/IL length ratio was 21.4 for ccTGA, 2.2 for transposition of the great arteries and 1.5 for normal hearts. The typical VSD in ccTGA is an outlet VSD. Its frequent misdiagnosis as an inlet VSD might be explained by the shortness of the inferior limb, which creates the illusion of a posterior VSD, and by the fact that the VSD is usually assessed from the left ventricular aspect. Surprisingly, the orientation of the septal band is similar in ccTGA and normal heart, despite the discordant atrioventricular connections, and different in ccTGA and transposition of the great arteries, despite the discordant ventriculo-arterial connections. These findings suggest that the mechanism leading to transposition in ccTGA and in TGA probably is different. The term 'double discordance' might therefore be more appropriate as a description of this complex anomaly.

Key words: cardiac anatomy; congenitally corrected transposition of the great arteries; discordant atrioventricular connections; discordant ventriculo-arterial connections; double discordance; septal band; ventricular septal defect.

Correspondence

Nicolas Arribard, Service de cardiologie pédiatrique, Hôpital universitaire des enfants Reine Fabiola, Avenue Jean Joseph Crocq 15, 1020 Bruxelles, Belgium. T: +32474307421; E: arribard.nicolas@gmail.com

Accepted for publication 5 September 2019

Introduction

Congenitally corrected transposition of the great arteries (ccTGA), or double discordance, is a rare congenital malformation. Its prevalence is estimated about 1/33 000 live

births, which represents approximately 0.5% of all congenital heart disease (Šamánek & Voříšková, 1999).

Congenitally corrected TGA associates discordant atrioventricular and ventriculo-arterial connections. Consequently, the morphologically left atrium communicates with the morphologically right ventricle (RV) through the tricuspid valve. The morphological right ventricle then communicates with the aorta. Conversely, the morphologically right atrium communicates with the morphologically left ventricle (LV) through the mitral valve. The morphological left ventricle then communicates with the pulmonary trunk. In consequence both discordant connections 'correct' themselves from a physiological standpoint, the systemic venous return flows towards the pulmonary trunk and the pulmonary venous return flows towards the aorta.

Although a ventricular septal defect (VSD) is frequently associated with the condition, in 75–80% of the cases, depending on the authors (Wallis et al. 2011), its anatomy remains controversial. The anatomical type of VSD has been variously described: perimembranous with inlet extension (Allwork et al. 1976), perimembranous outflow (subpulmonary) (Hornung & Calder, 2010), conoventricular (Van Praagh et al. 1998) and inlet (Kutty et al. 2018).

This VSD is a possible consequence of the malalignment between the atrial septum and the ventricular septum (Allwork et al. 1976). The observed difficulties in classifying this VSD could be due to the fact that, in the vast majority of ccTGA, the morphologically RV is left-sided, with apparent anatomical differences compared with a right-sided RV. In fact, when looking at the heart specimens, multiple questions arise: are the ventricles in the majority of ccTGA just mirror-imaged, or completely different from a normal heart? If they appear different, could this be the consequence of the discordant atrioventricular connections? If not, is this particular anatomy due to the L-loop or to the L-transposition of the great arteries, also present in the majority of ccTGA?

To try to answer these questions we have decided to compare the RV septal anatomy between ccTGA, transposition of the great arteries (TGA) and normal heart (NH), and to determine the anatomy of the VSD in ccTGA.

Materials and methods

Materials

Among the 1423 human postnatal heart specimens of the anatomical collection of the French Reference Centre for Complex Congenital Heart Defects (M3C), 31 had ccTGA. In addition, we examined eight fetal heart specimens with ccTGA from the M3C fetal heart collection. Among these 39 specimens, eight were excluded (all of them postnatal) because the septal band was not visible enough and could not therefore be analysed. The final ccTGA group therefore included 23 postnatal and eight fetal hearts. For comparison, 35 'normal hearts' (NH, 32 postnatal, 3 fetal) and 36 hearts with transposition of the great arteries (TGA, 36 postnatal) were also

analysed. The NH group was comprised of completely normal hearts and hearts with normal intracardiac anatomy (cardiomyopathy, persistent patency of the arterial duct or coronary arterial abnormalities). The NH and TGA specimens were selected according to the visibility of the septal band. Because of the technical difficulties in measuring the limbs of the septal band in hearts with TGA and outlet VSD, due to the frequent anterior malalignment of the outlet septum, we decided to include only TGA with intact ventricular septum, especially as the presence or not of a defect between the limbs of the septal band does not change its orientation and thus our measurements.

Methods

The heart specimens were reviewed and their anatomical characteristics were described according to segmental analysis (Van Praagh, 1972). We paid particular attention to the anatomy of the right ventricle, especially the anatomy of the outflow tract, the septal band and its two limbs, superior and inferior. Figure 1 shows the normal anatomy of the right ventricle in a normal heart.

We described the VSD according to the most recent classification of the International Society for Nomenclature of Paediatric and Congenital Heart Disease (ISNPCHD) for the 11th iteration of the International Classification of Disease (Franklin et al. 2017; Lopez

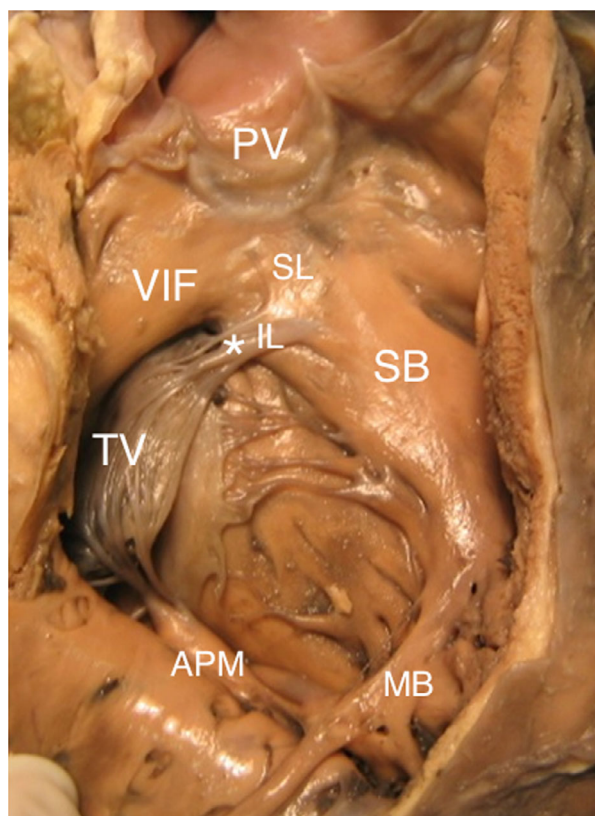


Fig. 1 Anatomy of the septal band on a normal heart specimen. APM, anterior papillary muscle of the tricuspid valve; IL, inferior limb of the septal band; MB, moderator band; PV, pulmonary valve; SB, septal band; SL, superior limb of the septal band; TV, tricuspid valve; VIF, ventriculo-infundibular fold; * medial papillary muscle.

et al. 2018). The VSD were defined by their location on the right ventricular side. An outlet VSD was defined by its location between the two limbs of the septal band, and above the superoseptal commissure of the tricuspid valve (Lopez et al. 2018). An inlet VSD was defined by its location below the inferior limb of the septal band and the medial papillary muscle and below the superoseptal commissure of the tricuspid valve, extending behind the entire length of the septal leaflet. A central perimembranous VSD was situated below and behind the inferior limb of the septal band and at the superoseptal commissure behind the septal leaflet of the tricuspid valve. Finally, a trabecular muscular defect was defined by its location within the apical muscular ventricular septum. In addition, and particularly for outlet defects, the fibrous or muscular nature of the postero-inferior border of the VSD was described.

Pictures of the septal band were taken with a μ Eye[®] camera and each picture included a ruler for length calibration. The camera was fixed, and the specimens were opened and exposed as orthogonally as possible to reduce parallax effect. We then analysed the pictures with PERFECT IMAGE[®] software.

Figure 2 shows how we performed the different measurements on a ccTGA specimen. First we drew a straight line (line A) following the upper side of the inferior limb of the septal band. Secondly, we drew a straight line (line B) following the inferior side of the superior limb of the septal band. Then we drew a third straight line (line C) between the two commissures of the arterial valve leaflet located just above the septal band (the pulmonary valve in normal heart and the aortic valve in TGA and ccTGA). This last measure was

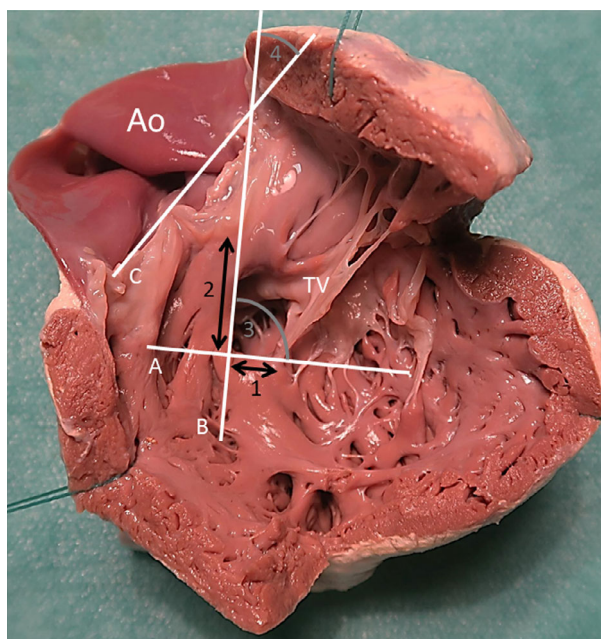


Fig. 2 Representation of the different measurements of the study on a ccTGA specimen. (A) Straight line following the upper side of the inferior limb of the septal band. (B) Straight line following the posterior side of the superior limb of the septal band. (C) Straight line between the two commissures of the arterial valve (aorta in ccTGA). 1: Length of the inferior limb of the septal band. 2: Length of the superior limb of the septal band. 3: Angle between the two limbs of the septal band. 4: Angle between the superior limb of the septal band and the arterial valve.

performed to determinate the global orientation of the septal band relative to the arterial valve. We used lines A and B to measure the length of the inferior limb and superior limb of the septal band. The length of the inferior limb (Measure 1) was measured between the crossing of lines A and B and the insertion of the medial papillary muscle. The length of the superior limb (Measure 2) was measured between the crossing of lines A and B and the crossing between line B and the arterial valve. We then measured the angle between the two limbs of the septal band (Measure 3) by measuring the angle between lines A and B. Finally, to estimate the global orientation of the septal band, we measured the angle between the superior limb of the septal band and the arterial valve (Measure 4) by measuring the angle between lines B and C.

All measures were carried out by the two main examiners (N.A. and L.H.).

We also noted whether the medial papillary muscle inserted terminally or laterally on the inferior limb of the septal band.

Statistical analysis

Statistical analysis was done with STATA[®] software. The Shapiro–Wilk test was done for normality, Student's *t*-test was used for comparison between parametric distributions and Mann–Whitney was used if at least one of the distributions was non-parametric. Statistical significance was assessed by using a cutoff *P*-value of 0.05.

Results

Segmental analysis

None of the specimens had heterotaxy. The majority of the heart specimens had usual atrial arrangement (Table 1). In the ccTGA group, 90% of the hearts were in atrial *situs solitus* (usual atrial arrangement), with L-loop ventricles and L-transposition of the great arteries {S,L,L}. Only one specimen (3%) in the TGA group and three specimens in NH group (9%) had an atrial mirror-imaged arrangement.

Associated lesions in ccTGA

Among the 31 ccTGA, 11 had pulmonary atresia and two had pulmonary stenosis. Seven had marked hypoplasia of the right ventricle. A straddling tricuspid valve was found in seven, and a straddling mitral valve in one. Five had Ebstein anomaly of the tricuspid valve.

Table 1 Anatomical characteristics of analysed specimens

	ccTGA	TGA	NH
Segmental analysis of the specimens	35 {S,L,L} 3 {I,D,D} 1 {S,L,D}	35 {S,D,D} 1 {I,L,L}	32 {S,D,S} 3 {I,L,I}
Total number of specimens analysed	39	36	35

Anatomy of the VSD in ccTGA

A VSD was present in 26/31 ccTGA (84%). The defect was an outlet VSD in 16 of the 26 VSD cases (61%), an inlet VSD in seven (27%) and a trabecular muscular VSD in one (4%). Two specimens had a confluent VSD extending from the outlet to the inlet (8%). There was no central perimembranous VSD. Among the 16 outlet VSDs, 10 had no malalignment of the outlet septum relative to the ventricular septum. The outlet septum was anteriorly malaligned below the pulmonary trunk in three specimens, and posteriorly aligned below the aorta in three. Among the 16 specimens with outlet defects, the postero-inferior rim of the

VSD was fibrous in 12 (outlet perimembranous VSD) and muscular in 4 (25%, outlet muscular VSD). Among the seven inlet VSDs, one was inlet muscular and six were inlet perimembranous. Figure 3 shows some examples, from the right and left ventricular side, of the various types of outlet and inlet VSD found in the group of ccTGA, according to the nature, fibrous or muscular, of their postero-inferior rim.

Septal band

The results of the different measurements are shown in Table 2. It is important to note that it was not always

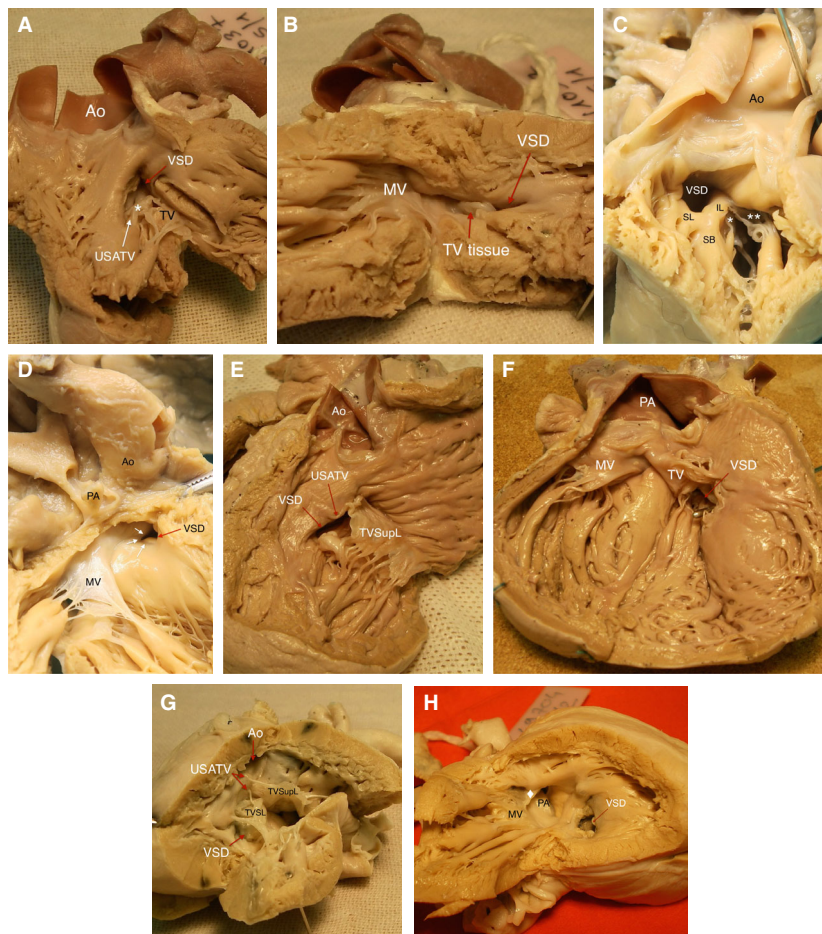


Fig. 3 The different types of outlet and inlet ventricular septal defects according to their borders. (A) Outlet perimembranous VSD, right ventricular view. The VSD is above the superoseptal commissure of the tricuspid valve. The asterisk indicates the fibrous postero-inferior rim of the defect. (B) Outlet perimembranous VSD, left ventricular view. (C) Outlet muscular VSD, right ventricular view. The VSD is above the upper septal attachments of the tricuspid valve. The postero-inferior border of the defect is muscular. (D) Outlet muscular VSD, left ventricular view. The white arrows indicate the muscular postero-inferior border of the defect. (E) Inlet perimembranous VSD, right ventricular view. The VSD is located below the superoseptal commissure of the tricuspid valve. The postero-inferior rim of the defect is fibrous. (F) Inlet perimembranous VSD, left ventricular view. The tricuspid valve straddles the inlet VSD. (G) Inlet muscular VSD, right ventricular view. The VSD is below the superoseptal commissure of the tricuspid valve, behind the septal leaflet of the tricuspid valve, and is closed by a patch. The postero-inferior border of the defect is muscular. (H) Inlet muscular VSD, left ventricular view. The VSD is closed by a patch. The borders of the defect are entirely muscular. *Septal leaflet of the tricuspid valve. ♦Subpulmonary fibrous diaphragm. **Superior leaflet of the tricuspid valve. IL, inferior limb of the septal band; PA, pulmonary artery; SB, septal band; SL, superior limb of the septal band; TV, tricuspid valve; TV tissue, tricuspid valve tissue, forming the fibrous postero-inferior rim of the defect; TVSL, septal leaflet of the tricuspid valve; USATV, upper septal attachments of tricuspid valve; VSD, ventricular septal defect.

Table 2 Comparison of measurements of the septal band between ccTGA, TGA and NH

	ccTGA	TGA	NH
Angle between the 2 limbs in degrees (number of specimens)*	76.4° (25)	90.6° (36)	76.1° (35)
Angle between superior limb and arterial valve in degrees (number of specimens)*	70.6° (31)	90.6° (36)	69.1° (35)
Ratio of the length of superior/inferior limbs (number of specimens)**	21.4 (31)	2.2 (36)	1.5 (35)

*The results were not statistically different between NH and ccTGA, but were different between NH and TGA, and between ccTGA and TGA.

**The results were not statistically different between NH and TGA, but were different between NH and ccTGA, and between ccTGA and TGA.

possible to do all the measurements in ccTGA specimens, due to the extreme shortness of the inferior limb of the septal band. In some specimens we arbitrarily decided to attribute a length of 0.1 mm to the inferior limb when it was too short to be measured. In these six cases the length ratio between the limbs and angle between the superior limb of the septal band and the arterial valve above could be measured, but not the angle between the two limbs. The numbers of specimens for each measurement are shown in Table 2.

The angle between the two limbs of the septal band was 76.4° in ccTGA and 76.1° in NH groups ($P = ns$). This angle was significantly different in TGA: 90.6° ($P = 0.003$ between NH and TGA, $P = 0.01$ between ccTGA and TGA).

The angle between the superior limb of the septal band and the arterial valve was 70.6° in ccTGA and 69.1° in NH ($P = NS$). Once again, this angle was significantly greater in TGA: 90.6° ($P < 0.001$ between NH and TGA, $P < 0.001$ between ccTGA and TGA).

The lengths of the two limbs of the septal band were very different among the specimens. This is due to the wide range of the size of the specimens, from foetal hearts to adult hearts. For this reason we decided to calculate the ratio between superior and inferior limbs of the septal band to estimate if one of them had a different length compared to the other one. This ratio was significantly higher in ccTGA : 21.4 vs. 2.2 in TGA ($P < 0.001$) and 1.5 in NH ($P < 0.001$), meaning that the inferior limb was shorter. However, this ratio was not significantly different between TGA and NH groups ($P = NS$).

Medial papillary muscle

The insertion of the medial papillary muscle was lateral in seven of 35 NH specimens, five of 36 TGA specimens and four of 30 ccTGA specimens ($P = NS$).

Discussion

Anatomy of the VSD

Ventricular septal defect (VSD) is described in the literature as a frequently associated lesion in ccTGA, especially in post-mortem studies. For Allwork et al. (1976) VSD, along with pulmonary obstruction and tricuspid valve malformations, is so frequent in ccTGA that it should be considered part of the malformation. Hornung, combining 22 anatomic cases with those of Allwork and Van Praagh, found, among 93 heart specimens, a VSD prevalence of 84% (Allwork et al. 1976; Van Praagh et al. 1998; Hornung & Calder, 2010). Our results are exactly similar, with 84% of our specimens having a VSD. However, the fact that these studies, including ours, were performed on cardiac specimens might lead one to conclude a higher rate of VSD because of the severity of the cases. Indeed, the prevalence of VSD is lower in foetal ultrasound studies (62%, Sharland et al. 2005) and clinical studies (72%, Rutledge et al. 2002). As some patients with ccTGA may be asymptomatic for a long period of time (Roffi et al. 1998), the real prevalence of associated VSD might even be lower than described.

The difficulties in classifying and naming the VSD in ccTGA were certainly related with the controversies which have lasted for years about the classification of VSD as a whole, but also, when the morphologically RV is left-sided, with the mirror-imagery of the ventricular mass itself. The determining feature of an outlet defect is that it always opens to the right ventricle between the limbs of the septal band (Mostefa-Kara et al. 2015). However, we have demonstrated that the inferior limb of the septal band is often very short in ccTGA and difficult to recognize on the right ventricular septal surface. We therefore used as a complementary anatomical landmark the attachments of the superoseptal commissure of the tricuspid valve, which is always situated on the inferior limb of the septal band. Using these two criteria, we could affirm that the VSD was an outlet VSD, located between the two limbs of the septal band, in 61% of our ccTGA cases with VSD. One of the factors explaining the difficulties in classifying the VSD in ccTGA is probably the malalignment between the atrial and ventricular septa (Anderson et al. 1974). This malalignment disturbs the anatomy of the conduction system and of the pulmonary trunk (Hosseinpour et al. 2004) and has been considered a direct cause of the presence of a VSD (Allwork et al. 1976), despite the fact that this malalignment also exists in ccTGA with an intact ventricular septum. As a consequence of this malalignment, the membranous septum, which is usually found in the region of confluence between atrial and ventricular septum, has no interventricular component anymore and separates the left atrium from the left ventricle, filling the gap between the malaligned atrial and ventricular septa, and separated from the mitral valve by the atrial septum (Fig. 4). This explains why we did not find

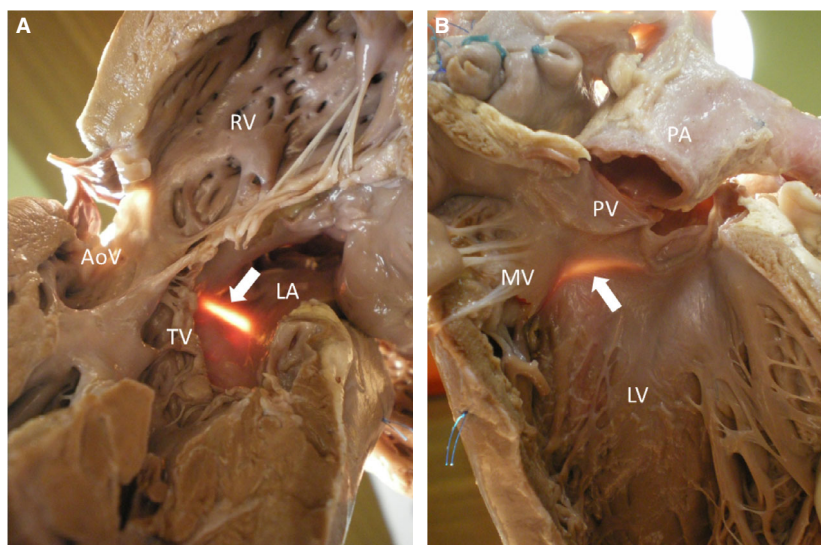


Fig. 4 Anatomy of the membranous septum in a ccTGA specimen. (A) View of the membranous septum from left atrium. The membranous septum is trans-illuminated from the left atrium. (B) View of the membranous septum from left ventricle. The membranous septum is trans-illuminated from the left atrium. →, membranous septum; AoV, aortic valve; LA, left atrium; LV, left ventricle; MV, mitral valve; PA, pulmonary artery; PV, pulmonary valve; RV, right ventricle; TV, tricuspid valve.

any central perimembranous VSD in our series. However, in the literature, the VSD in ccTGA is often considered an inlet VSD. We found that the inferior limb of the septal band was much shorter in ccTGA than in TGA and NH, and can almost disappear. This can easily create the illusion of a posterior VSD and might be a reason for its frequent misdiagnosis as an inlet VSD. Another reason for that misdiagnosis is that the anatomy of the VSD in ccTGA is often assessed from the stance of the usually right-sided left ventricle.

The septal band and the inner architecture of the right ventricle

The differences between ccTGA and NH relative to the morphology of the left ventricle have been well described (Allwork et al. 1976; Wallis et al. 2011). However, the precise anatomy of the right ventricle in ccTGA has not been thoroughly studied. The right ventricle has been described as almost always smaller (Anderson et al. 1978), due to hypoplasia of the RV sinus (Van Praagh et al. 1998). However, its structure is not described as really different from a normal heart, with a subarterial (subaortic in this case) conus, a prominent septal band which ‘bifurcates superiorly as in the normal right ventricle’, with the medial papillary muscle (or a ‘tendinous cord’) arising from its inferior limb (Allwork et al. 1976). Yet, when we look at the specimens, the left-sided right ventricle in ccTGA does not look quite the same as in a normal heart. The main anatomical structures are present, but the septal band is sometimes more difficult to individualize. This aspect looks similar in hearts in *situs inversus totalis* (complete mirror image). We wanted to assess with objective measurements whether there was any

morphological difference in the inner anatomy of the right ventricle between NH and ccTGA. If no difference was notable, it could mean that the L-loop itself would not be sufficient to create this abnormal aspect, and that the reason for it could be the discordant atrioventricular connections. We found that the angle between the two limbs of the septal band and the orientation of the septal band itself are similar but mirror-imaged between NH and ccTGA (Fig. 4A, B). This might suggest that the anatomy of the right ventricular septal surface might indeed not be as abnormal that it seems, despite the L-loop.

It would be of great interest to compare the orientation of the septal band in hearts in usual atrial arrangement and in atrial mirror-imaged arrangement in the three groups (ccTGA, TGA and NH). Unfortunately, the number of specimens with atrial mirror-imaged arrangement in each group is too small to allow for comparison. Magnetic resonance tagging studies in patients with normal hearts in usual and mirror-imaged arrangement have demonstrated that even if the gross anatomy is mirror-imaged in hearts with *situs inversus*, especially at the basal part of the two ventricles, the packing of cardiomyocytes at the LV apex and the LV apical deformation is not mirror-imaged in these hearts (Delhaas et al. 2008). Cardiomyocyte organization studies were done by Asami on two specimens with ccTGA and showed that packing of the cardiomyocytes in the left ventricle followed the same clockwise course seen in normal hearts, and that no mirror-imaged arrangement was found in the deep layers of the left ventricular wall (Asami & Koizumi, 1989). Some explanations could be that genomic control of left/right development is not the only factor determining the orientation of cardiomyocyte packing,

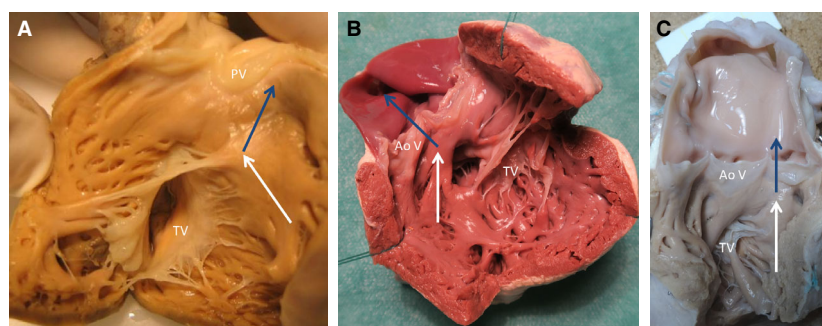


Fig. 5 Typical orientation of the right ventricular outflow tract in NH, ccTGA and TGA specimens. The white arrows are positioned over the septal band, and the blue arrows are positioned along the axis of the vessel originating from the right ventricle. (A) View of the right ventricular outflow tract in NH. (B) View of the right ventricular outflow tract in ccTGA. (C) View of the right ventricular outflow tract in TGA. AoV, aortic valve; PV, pulmonary valve; TV, tricuspid valve.

other factors as mechanical forces might also play a role (Delhaas et al. 2008). Even if these studies were performed only on morphologically left ventricles and not on morphologically right ventricles, some questions arise: how is the packing of the cardiomyocytes in a right ventricle? Even if the RV gross anatomy in ccTGA seems to be mirror-imaged, are the cardiomyocytes normally oriented as in LV? The analysis of the orientation of cardiomyocyte packing in the right ventricle, in particular the comparison between NH and ccTGA, seems to be a particularly interesting future field of research.

It is well known that the orientation of the ventricular septum is not the same in TGA and in NH. In the normal heart, the RV outflow tract is oriented at an acute angle to the left ventricular outflow tract (Delhaas et al. 2008). In TGA, the vessels run parallel to each other and the RV outflow tract is oriented parallel to the LV outflow tract. Therefore, the upper part of the right side of the ventricular septum is straight instead of twisted (Chiu et al. 1984; Kurosawa & Van, 1986). This may be due to the absence of rotation of the outflow tract during cardiac development (Bajolle et al. 2006).

The myocardium of the outflow tract is involved in normal positioning of the great arteries. During heart development, the aortic valve rotates anticlockwise to reach the mitral valve and to wedge between the mitral and the tricuspid valve, resulting in spiraling great arteries. The absence of this rotational mechanism in TGA was first described anatomically (Lomonico et al. 1988) and then using transgene detection (Bajolle et al. 2006). The absence of rotation leads to a different anatomy of the interventricular septum between NH and TGA. The interventricular septum is more straightforward in TGA than in NH. This is confirmed by our results, which demonstrate a significant difference between NH and TGA in the angle between the two limbs of the septal band and the orientation of the septal band itself (Fig. 5A,C). The septal band is located in the right ventricular outflow tract region and might therefore be impacted by the presence or absence of this rotational

mechanism. Further investigations are required to confirm this hypothesis.

What was unexpected was that the orientation of the septal band is exactly similar in NH and in ccTGA, despite the fact that in ccTGA the ventriculo-arterial connections are discordant. Indeed, we found a significant difference in the angle between the two limbs of the septal band and the orientation of the septal band itself between ccTGA and TGA, although they both have discordant ventriculo-arterial connections and parallel great arteries. The ventricular septum in ccTGA is not straight, contrary to TGA. In other words, in ccTGA, the vessels but not the outflow tracts are parallel, in contrast to TGA, where both the vessels and the outflow tracts are parallel (Fig. 5B,C). This raises several questions: is the transposition of the great arteries different in ccTGA and in TGA? Is the transposition in ccTGA also due to a lack of rotation of the outflow tract or is it due to a different developmental mechanism?

These anatomical findings may have clinical implications. It is well known that patients with systemic right ventricle in TGA palliated by atrial switch and patients with systemic right ventricle in ccTGA have different outcomes (Brida et al. 2018). The differences observed in RV anatomy might play a role in the dysfunction of the systemic right ventricle, which occurs earlier in TGA post-atrial switch than in ccTGA (Grothoff et al. 2013).

Concerning the insertion of the medial papillary muscle, no difference was found between the three groups. It has already been described that the position of the medial papillary muscle was inconstant in NH (Restivo et al. 1989), and it seems to be the same for TGA and ccTGA.

Limitations of the study

The principal limitation of this study is the small number of heart specimens. There is a selection bias in the heart collection; specimens with more severe disease are overrepresented. The study groups are very heterogeneous in terms of age and hence size of the heart. The conservation

method (10% formaldehyde solution) does not alter significantly the morphometric parameters of the specimens (Holda et al. 2016). However, the manipulation of the specimens for teaching purposes might have influenced the heart anatomy. Due to the measurement method, a parallax effect cannot be totally excluded. All possible efforts to avoid it were made and the residual effect, if any, should affect the three groups equally.

Conclusion

We confirmed that VSD is a frequently associated lesion in ccTGA and that it opens in the outlet of the RV in most cases. The orientation of the limbs of the septal band, which are part of the outflow tract of the right ventricle, seems to be identical but mirror-imaged between NH and ccTGA despite their different atrioventricular connections, and different between ccTGA and TGA despite their common discordant ventriculo-arterial connections. The difference between NH and TGA is probably an anatomical consequence of the lack of rotation of the outflow tract in TGA. The difference between ccTGA and TGA suggests that different mechanisms leading to transposition might be involved in ccTGA and TGA.

This anatomical study confirms that the major feature of ccTGA is the discordant nature of the atrioventricular connections, not the nature of the ventriculo-arterial connections. From a nomenclature and classification standpoint, this implies that ccTGA should no longer be considered a variant of TGA. The term 'double discordance', used in French but which easily transposed into English, might therefore be more appropriate to describe this complex anomaly.

Acknowledgements

Grants: Nicolas Arribard was granted a grant by the Bourse de recherche de la Filiale de Cardiologie Pédiatrique et Congénitale (FCPC) 2018 of the French Cardiac Society (SFC).

Conflict of interest

The authors have no conflict of interest to declare.

Author contributions

N.A. and L.H. took the measurements and drafted the manuscript. M.M., S.H. and D.B. contributed to specific sections and made critical revisions for intellectual content. B.B. prepared the fetal cardiac specimens. All authors have read and approved the final manuscript.

References

Allwork SP, Bentall HH, Becker AE, et al. (1976) Congenitally corrected transposition of the great arteries: morphologic study of 32 cases. *Am J Cardiol* **38**, 910–923.

Anderson RH, Becker AE, Arnold R, et al. (1974) The conduction tissues in congenitally corrected transposition. *Circulation* **50**, 911–923.

Anderson KR, Danielson GK, McGoon DC, et al. (1978) Ebstein's anomaly of the left-sided tricuspid valve: pathological anatomy of the valvular malformation. *Circulation* **58**, 187–191.

Asami I, Koizumi K (1989) The vortex cordis is never reversely directed, even in situs inversus and L-loop anomaly. *Kaibogaku Zasshi* **64**, 36–45.

Bajolle F, Zaffran S, Kelly RG, et al. (2006) Rotation of the myocardial wall of the outflow tract is implicated in the normal positioning of the great arteries. *Circ Res* **98**, 421–428.

Brida M, Diller GP, Gatzoulis MA, et al. (2018) Systemic right ventricle in adults with congenital heart disease: anatomic and phenotypic spectrum and current approach to management. *Circulation* **137**, 508–518.

Chiu S, Anderson RH, Macartney FJ, et al. (1984) Morphologic features of an intact ventricular septum susceptible to subpulmonary obstruction in complete transposition. *Am J Cardiol* **53**, 1633–1638.

Delhaas T, Kroon W, Bovendeerd P, et al. (2008) Left ventricular apical torsion and architecture are not inverted in situs inversus totalis. *Prog Biophys Mol Biol* **97**, 513–519.

Franklin RC, Béland MJ, Colan SD, et al. (2017) Nomenclature for congenital and paediatric cardiac disease: the International Paediatric and Congenital Cardiac Code (IPCCC) and the Eleventh Iteration of the International Classification of Diseases (ICD-11). *Cardiol Young* **27**, 1872–1938.

Grothoff M, Fleischer A, Abdul-Khalig H, et al. (2013) The systemic right ventricle in congenitally corrected transposition of the great arteries is different from the right ventricle in dextro-transposition after atrial switch: a cardiac magnetic resonance study. *Cardiol Young* **23**, 239–247.

Holda MK, Klimek-Piotrowska W, Koziej M, et al. (2016) Influence of different fixation protocols on the preservation and dimensions of cardiac tissue. *J Anat* **229**, 334–340.

Hornung TS, Calder L (2010) Congenitally corrected transposition of the great arteries. *Heart* **96**, 1154–1161.

Hosseinpour AR, McCarthy KP, Griselli M, et al. (2004) Congenitally corrected transposition: size of the pulmonary trunk and septal malalignment. *Ann Thorac Surg* **77**, 2163–2166.

Kurosawa H, Van LM (1986) Surgical anatomy of the infundibular septum in transposition of the great arteries with ventricular septal defect. *J Thorac Cardiovasc Surg* **91**, 123–132.

Kutty S, Danford DA, Diller GP, et al. (2018) Contemporary management and outcomes in congenitally corrected transposition of the great arteries. *Heart* **104**, 1148–1155.

Lomonico MP, Bostrom MP, Moore GW, et al. (1988) Arrested rotation of the outflow tract may explain tetralogy of Fallot and transposition of the great arteries. *Pediatr Pathol* **8**, 267–281.

Lopez L, Houyel L, Colan SD, et al. (2018) Classification of ventricular septal defects for the eleventh iteration of the international classification of diseases – striving for consensus: a report from the International Society for Nomenclature of Paediatric and Congenital Heart Disease. *Ann Thorac Surg* **106**, 1578–1589.

Mostefa-Kara M, Bonnet D, Belli E, et al. (2015) Anatomy of the ventricular septal defect in outflow tract defects: similarities and differences. *J Thorac Cardiovasc Surg* **149**, 682–688.

Restivo A, Smith A, Wilkinson JL, et al. (1989) The medial papillary muscle complex and its related septomarginal

- trabeculation. A normal anatomical study on human hearts. *J Anat* **163**, 231.
- Roffi M, De Marchi SF, Seiler C** (1998) Congenitally corrected transposition of the great arteries in an 80 year old woman. *Heart* **79**, 622–623.
- Rutledge JM, Nihill MR, Fraser CD, et al.** (2002) Outcome of 121 patients with congenitally corrected Transposition of the great arteries. *Pediatr Cardiol* **23**, 137–145.
- Šamánek M, Voříšková M** (1999) Congenital heart disease among 815,569 children born between 1980 and 1990 and their 15-year survival: a prospective Bohemia survival study. *Pediatr Cardiol* **20**, 411–417.
- Sharland G, Tingay R, Jones A, et al.** (2005) Atrioventricular and ventriculoarterial discordance (congenitally corrected transposition of the great arteries): echocardiographic features, associations, and outcome in 34 fetuses. *Heart* **91**, 1453–1458.
- Van Praagh R** (1972) The segmental approach to diagnosis in congenital heart disease. *Art Ser* **8**, 4–23.
- Van Praagh R, Papagiannis J, Grünenfelder J, et al.** (1998) Pathologic anatomy of corrected transposition of the great arteries: medical and surgical implications. *Am Heart J* **135**, 772–785.
- Wallis GA, Debich-Spicer D, Anderson RH** (2011) Congenitally corrected transposition. *Orphanet J Rare Dis* **6**, 22.